CHAPTER 9

ROLE OF THE GREENLAND-SCOTLAND RIDGE IN NEOGENE CLIMATE CHANGES

James D. Wright

Cenozoic climates are marked by long-term cooling since the early Eocene that evolved into the large amplitude glacial/interglacial cycles of the late Pleistocene. Circulation models (both atmospheric and oceanic) have simulated these changes by altering the concentration of atmospheric trace gases (i.e., increased CO_2) or by changing the meridional heat transports (increased delivery of heat to the poles via oceanic circulation) (e.g., Barron, 1983, 1987; Manabe and Bryan, 1985; Rind, 1987; Covey and Barron, 1988; Covey and Thompson, 1989; Manabe et al., 1990; Rind and Chandler, 1991). There is evidence in support of both mechanisms, leaving unclear the fundamental cause of the long-term climate change during the Cenozoic. Identifying mechanisms that triggered Cenozoic cooling has focused on tectonic changes, both marine and terrestrial, that fundamentally altered the ocean-atmosphere system. Arrangements of continents and marine gateways dictate surface and deep-water circulation patterns, and therefore, how water masses communicate between the ocean basins. Opening of the Drake Passage and uplift of the Central American Isthmus are two gateways that are often associated with climate change. The Drake Passage gateway is thought to be a critical "valve" in the development of a circumpolar circulation that led to the thermal isolation of Antarctica (Kennett, 1977). The closure of the Central American Isthmus has been implicated as a potential causes for large-scale Northern Hemisphere glaciation (Keigwin, 1982) and the formation of deepwater in the North Atlantic (Keigwin, 1982; Maier-Reimer et al., 1990). The Greenland-Scotland Ridge is such a gateway, separating the cold, polar water masses in the Greenland–Norwegian Seas and Arctic Ocean from the open Atlantic. Thus, the opening and closing of this gateway may provide a critical control on long-term climates.

Today, much of the Greenland-Scotland Ridge is less than 500 m deep, making the water depths across this marine connection sensitive to small vertical changes through either tectonic or eustatic processes. At present, surface and intermediate/deep waters are exchanged between the Nordic seas and open North Atlantic. Vogt (1986) termed the Greenland-Scotland Ridge a "watergate" that acts as a valve for the exchange of water across the ridge. Warmer waters from the North Atlantic Current flow into the Norwegian Sea, while cold polar surface waters flow to the south along the Greenland coast as part of the East Greenland Current (Worthington, 1970; Aagaard, 1982; Swift, 1984, 1986). This sets up an asymmetric circulation pattern from the southwest to the northeast. Intermediate to deep waters flow from the Norwegian-Greenland Seas over the Greenland-Scotland Ridge mainly through three passages: Denmark Straits with a sill depth of ~620 m; Iceland-Faeroe Ridge with a sill depth of ~500 m, and Faeroe Bank Channel with a sill depth between 800 and 900 m (Fig. 9.1) (Worthington, 1970). Once in the North Atlantic, these waters eventually combine with Labrador Sea Water to form North Atlantic Deep Water (NADW). This deep current in the modern ocean flows south to the Southern Ocean where its waters are distributed throughout the world's ocean (Gordon, 1981).

Changes in North Atlantic thermohaline circulation have been an integral part of many climate change hypotheses (e.g., Broecker and Denton, 1990). Indeed, there is a good correlation between deepwater circulation patterns in the North Atlantic and climate change (e.g., Boyle and Keigwin, 1987; Raymo et al., 1990, 1992; Jansen

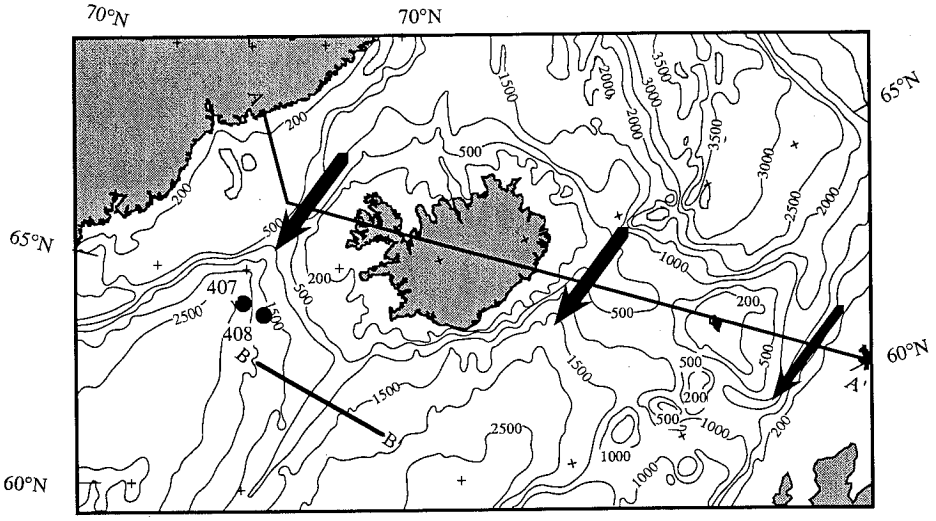

Fig. 9.1. Bathymetry of the northern North Atlantic and Greenland and Norwegian Seas surrounding Iceland (redrawn from *Tucholke et al.*, 1986). The contour interval is 500 m, except for a 200 m contour. Note the shallow depths associated with features proximal to Iceland. Profiles A to A' and B to B' mark cross sections across the Greenland-Scotland and Reykjanes Ridges, respectively shown in Figure 9.2. The large black arrows mark channels where deep water masses overflow into the North Atlantic.

and Veum, 1990; Charles and Fairbanks, 1992; Keigwin et al., 1991, 1994; Lehman and Keigwin, 1992; Oppo and Lehman, 1993; Keigwin and Jones, 1994; Keigwin and Lehman, 1994). One possible link between North Atlantic thermohaline circulation and climate is that higher latitude regions are strongly influenced by the heat released from the ocean during convection. In particular, there is a significant amount of heat released with the formation of NADW (Broecker and Denton, 1990) which is responsible for the relatively warm climates of western Europe and Scandinavia. Furthermore, the upwelling of NADW in the Southern Ocean is an important source of heat for the seasonal meltback of sea ice in the Southern Ocean (Gordon, 1981; Jacobs et al., 1985).

Long-term changes in Northern Component Water (NCW, analogous to modern NADW)[1] production may be related to sill depth changes along the Greenland-Scotland Ridge. The Greenland-Scotland Ridge system is ~3000 km in length, but less than one half of this length is presently deeper than 200 m, and only 300 km is deeper than 500 m (Fig. 9.1). The relatively shallow depths of the Greenland-Scotland Ridge are associated with the Iceland mantle plume now centered under east central Iceland (Vogt, 1971, 1983; Vogt and Avery, 1974; Nunns, 1983). A large regional swell from the mantle plume extends radially away from Iceland for about 1000 km (Anderson et al., 1973; Vogt et al., 1981; Schilling, 1986; White and McKenzie, 1989; Sleep, 1990). This regional swell results from the injection of heat and buoyant mantle material into the asthenosphere below the crust (White and McKenzie, 1989; Sleep, 1990). The low density and thick crust of the Greenland-Scotland Ridge also contributes to the shallow depths of this gateway. Crustal thicknesses of 30 km are thought to underlie the Iceland-Faeroe Ridge (Bott, 1983). Recent evidence indicates that crustal thicknesses under Iceland are greater than 20 km (White et al., 1996). The isostatic adjustment to this thick, but low density crust (relative to the mantle below) causes the Greenland-Scotland Ridge to be a bathymetric high, sitting well above the surrounding seafloor.

[1]Because NADW by definition has specific water mass properties, the term Northern Component Water is used to designate the North Atlantic Deep Water mass that may have formed by similar processes in the past, but with different physical-chemical properties (Broecker and Peng, 1982).

Figure 1.

The mantle plume and the crustal thickness and density affect the long-term depths of the Greenland-Scotland Ridge in different ways. Accordingly, there are two general models for Greenland-Scotland Ridge subsidence. One model suggests that the Greenland-Scotland Ridge behaved like normal ocean crust throughout its history and subsided at a rate proportional to the square root of the age of the crust (e.g., Thiede and Eldholm, 1983). Even though the crust is anomalously thick, thermal subsidence will continue as the newly formed material moves laterally away from the mantle plume. These simple thermal contraction subsidence models minimize any changes in the mantle plume activity, favoring long-term thermal subsidence as the dominant control on ridge depths. In contrast, others have suggested that the Greenland-Scotland Ridge has had a more variable history that was tied to changes in the mantle plume flux through time (Vogt, 1972, 1983; Shor and Poore, 1979; Wright and Miller, 1996). These studies indicate that the regional swell has varied in horizontal extent and elevation during the Neogene, and hence, has affected the exchange of water masses between the Greenland-Norwegian Seas and the northern North Atlantic. In this chapter, the evidence and implications for both the simple and more dynamic models of thermal subsidence on the Greenland-Scotland Ridge are reviewed to evaluate the role that this marine gateway has played in Neogene climate change.

Greenland-Scotland Ridge Tectonics

Plume volcanism on what is now Iceland produced the thick crust which forms the Greenland-Scotland Ridge today. Lateral movement from seafloor spreading has carried this crust away from the spreading center, producing the ridge. As product of the oceanic spreading system, the Greenland-Scotland Ridge should have a predictable thermal subsidence (Sclater et al., 1971; Berger and Winterer, 1974):

$$d = id + k\sqrt{t} - s \qquad (9.1)$$

where d is the predicted depth (m), id is the initial depth (m) at the ridge, k is 300, empirically derived for the North Atlantic by *Miller et al.* (1987), t is the age of the crust, and S is a correction for sediment thickness. For the Greenland-Scotland Ridge, simple thermal subsidence models indicate that the ridge reached a critical depth as early as the late early Miocene (~17 Ma) (Vogt, 1972) or during the middle Miocene (~14 Ma) (Schnitker, 1980; Thiede and Eldholm, 1983). The "critical" depth is defined as the depth that allowed both surface and deep water to exchange between the northern North Atlantic and Norwegian-Greenland Seas. Vogt (1972) and Schnitker (1980) cited paleoceanographic evidence supporting their interpretation of when subsidence of the ridge reached the critical depth.

The dynamic mantle plume hypothesis was first postulated by Vogt (1971) based on the step-like appearance of several bathymetric (basement) features along the Reykjanes Ridge (Talwani et al., 1971). Vogt identified five major features on each side of the Reykjanes Ridge, Escarpments E and A and Ridges B, C, and D, that were coherent along much of the ridge's length (Fig. 9.2). Escarpments E and A are the largest of these features and have 500–800 m of vertical relief. The observed crustal depths in this region, particularly for the features identified by Vogt (1971), are generally less than those predicted by simple thermal subsidence. The higher topography can be produced thermally through a hotter mantle and/or volumetrically through increased melting and crustal thickening. These features were attributed to fluctuations in plume activity under Iceland that propagated along the ridge axis (Vogt, 1971, 1983). The flux of mantle material along the Reykjanes Ridge is time-transgressive, creating a V-shaped signature (Vogt, 1971, 1983; White et al., 1995). Large variations in water depths indicate that the mantle plume activity under Iceland has not been constant during the Neogene. Vogt used the age versus distance relationships of the escarpments and ridges to estimate that the propagation rate of mantle material along the ridge was ~20 cm/yr. Using this rate, the mantle plume events that formed Escarpments E and A originated under Iceland at ~17 and 7 Ma, respectively.

Two studies (Johansen et al., 1984; Wright and Miller, 1996) have re-analyzed the geophysical data from cruise Vema 23-03 (Talwani et al., 1971). Wright and Miller (1996) estimated that the mantle plume event that created Escarpment E originated around 16.3 Ma, similar to Vogt's estimate. However, their age estimate for the base of

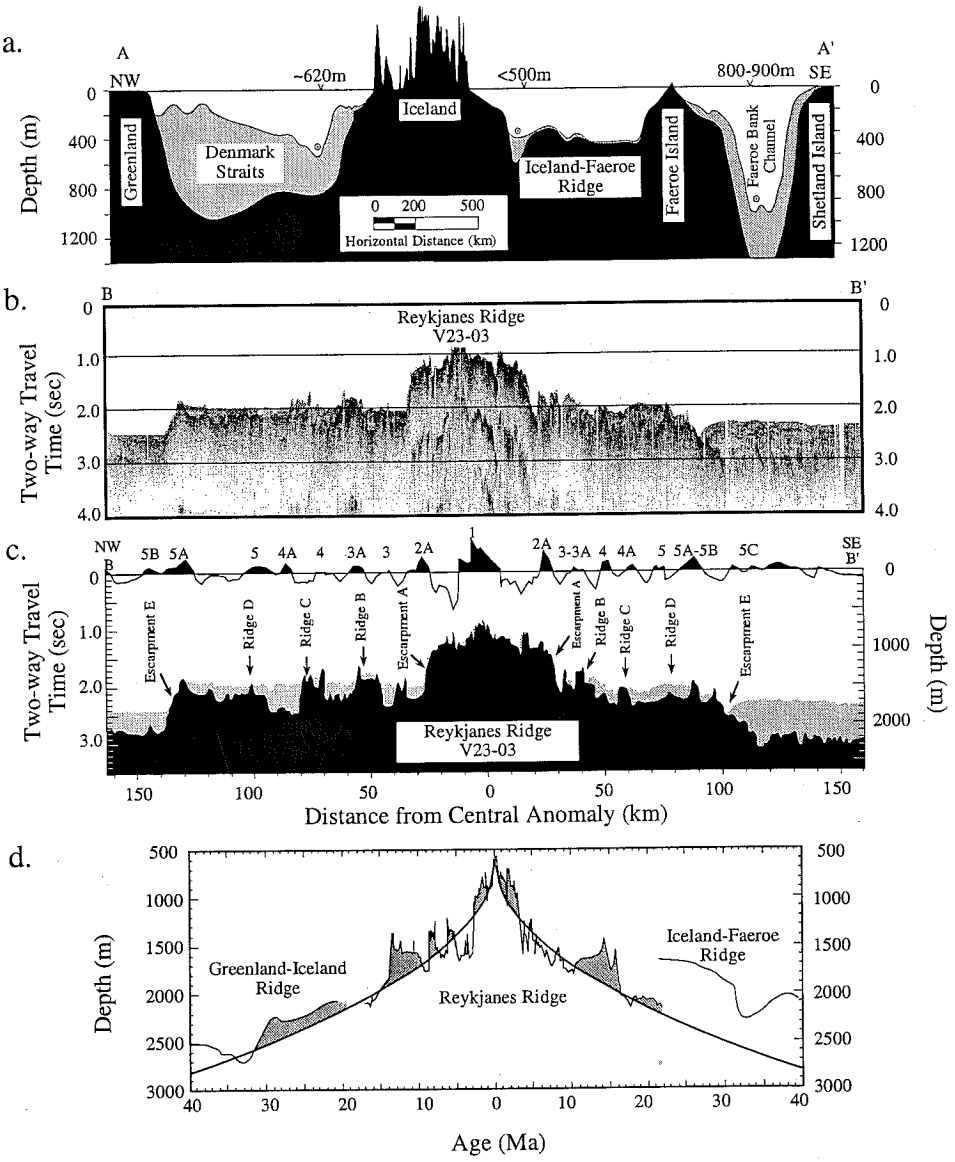

Fig. 9.2. The A-A' cross section shows the Greenland-Scotland Ridge (a, adapted from *Miller and Tucholke*, 1983). Sediment coverage is shaded in gray. The main conduits of water across the GSR are marked by circles: the Denmark Strait (~600 m), on the Greenland–Iceland segment of the GSR, the Iceland-Faeroe overflow where water depths are ~500 m, and the Faeroe Bank Channel between the Faeroe Islands and Shetland Island. The GSR overflow to the east and west of Iceland is roughly equal. (b) Seismic line across the Reykjanes Ridge shown in Figure 9.1 (B - B'). (c) Interpretation of V23-03 seismic transect across the Reykjanes Ridge. *Vogt* (1971) identified several coherent bathymetric features along the Reykjanes Ridge (Escarpments E and A; Ridges D, C, B) attributed these to changes in the Icelandic mantle plume discharge. The polarity patterns across the Reykjanes Ridge are shown above the cross section. Numbers above the polarity patterns represent anomaly numbers. (d) Crustal depths versus age for the Reykjanes and GSR were adjusted to account for the effects of sediment loading. The smooth curve radiating from 0 Ma is the predicted thermal subsidence curve which used a decay of $300\sqrt{t}$. The initial starting depth used for this section across the Reykjanes Ridge was 600 m. The initial depth used for the GSR and Iceland-Faeroe Ridge was 1100 m above sea level. The difference between the GSR/Iceland Faeroe Ridge and Reykjanes Ridge initial depths is 1700m and this value was subtracted from the GSR and Iceland Faeroe cross sections to compare to the Reykjanes Ridge cross section. Time when the crust was higher than the predicted depth are shaded in gray.

Figure 2.

Escarpment A was closer to 4 Ma, not 7 Ma as Vogt suggested, indicating a much higher propagation rate of the anomaly along the ridge axis for the younger event. Wright and Miller (1996) proposed that the plume discharge for the older events encountered a colder asthenosphere, slowing the progression of the anomaly away from the source. The discharge from each successive event encountered a hotter asthenosphere and less resistance, allowing faster propagation of the thermal or melting anomaly along the Reykjanes system. To estimate the chronologies for the plume events on Iceland, Wright and Miller (1996) applied a linear regression to the age versus distance (from Iceland) relationship for each event on each Reykjanes Ridge crossing (see Fig. 3 in Wright and Miller, 1996). The zero-distance intercept for each regression should reflect the timing of each mantle plume event under Iceland (e.g., Vogt, 1971).

Depths along the Reykjanes Ridge may provide the most complete proxy record for mantle plume variations; however, additional evidence from Iceland is consistent with variations in mantle plume fluxes. The Iceland Plateau is covered by successive and thick (3–4 km) sequences of lava flows that have accumulated during the last 15 million years. Rates of accumulation of lava sequences on Iceland are well-constrained by K-Ar dates (Saemundsson et al., 1980; McDougall et al., 1984; Saemundsson, 1986) and indicate higher accumulation rates (> 2 km/m.y.) in some lava flows. Intervals of higher rates of lava accumulation occurred between 14 and 12 Ma, 9.5 and 9.0 Ma, and 7.5 and 6.5 Ma (Fig. 9.3). These intervals correspond to intervals of higher mantle plume activity inferred from the Reykjanes Ridge. While the timing between the changes on the Reykjanes Ridge and high lava accumulation is compelling, these records of volcanism on Iceland are incomplete, making it difficult to characterize the volcanic history on Iceland from a succession of lava flows.

Regional mantle plume activity might also be recorded by the volcanic ash layers in marine sediments proximal to the Icelandic Plateau. Deep Sea Drilling Project Sites (DSDP) 407 and 408 were drilled to the south of the Iceland Plateau, while Ocean Drilling Program (ODP) Site 907 was drilled to the north of the plateau (Fig. 9.1) with each site containing substantial volcanic material (Luyendyk et al., 1979; Myhre et al., 1995). The origin of the volcanic sediments is not constrained but the overall pattern of high ash accumulation indicates relatively high regional volcanism through much of the Miocene (Fig. 9.3). Several ash layers deposited during the middle and late Miocene appear to correspond with the development of Escarpment E and Ridges D and C; however the overall pattern of ash deposition is equivocal concerning times of increased mantle plume activity.

Deep Water Circulation

First-order deepwater circulation patterns during the Neogene have been well-established through various proxies (Jones et al., 1970; Ruddiman, 1972; Shor and Poore, 1979; Schnitker, 1980; Miller and Tucholke, 1983; Miller and Fairbanks, 1985; Vogt and Tucholke, 1989; Woodruff and Savin, 1989; Wright et al., 1991, 1992; Wold, 1994; Wright and Miller, 1996). There is general agreement concerning long-term NCW production from the late middle Miocene (12 Ma) to Present. Many studies have recognized that the most recent phase of NCW production began in the late middle Miocene and has continued with minor interruptions until the present (e.g., Shor and Poore, 1979; Schnitker, 1980; Miller and Fairbanks, 1985; Woodruff and Savin, 1989; Wright et al., 1991; 1992; Wold, 1994; Wright and Miller, 1996). The interpretation of early to early middle Miocene deepwater circulation patterns in the North Atlantic is more controversial with some studies questioning the existence of NCW prior to the middle Miocene (cf., Woodruff and Savin, 1989; Wright et al., 1992).

One of the best tools for inferring past deepwater circulation patterns is carbon isotope records from the deep ocean. In the modern ocean, there are considerable differences in dissolved inorganic carbon (DIC) $\delta^{13}C$ values, reflecting the basin-to-basin fractionation caused by deepwater circulation patterns (Kroopnick, 1985). This fractionation occurs because the $\delta^{13}C$ value and nutrient content of deep/bottom waters is a function of the time the water mass has been isolated from the surface. As water masses sink and move away from their source regions, organic matter falling from the surface ocean collects at depth. Oxidation of this organic matter releases CO_2 with low $\delta^{13}C$ values (-25‰) and high nutrients, lowering the DIC $\delta^{13}C$ value in the deep

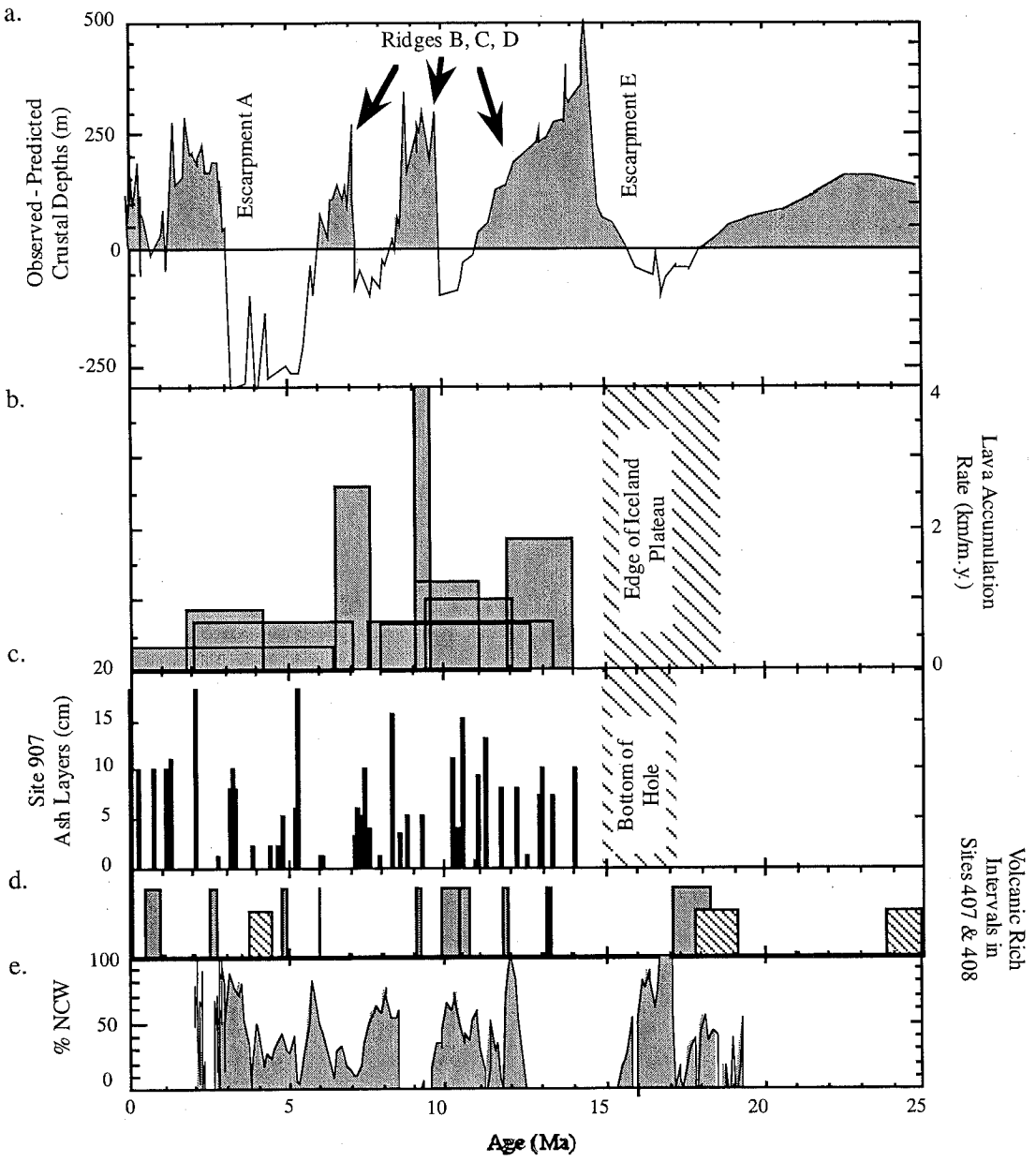

Fig. 9.3. (a) Difference curve between the observed and predicted crustal depths for the Reykjanes and GSR cross sections shown in Figure 9.2d. The chronology of the Reykjanes portion of this record has been adjusted so that Escarpments E and A and Ridges D, C, and B have the ages inferred by *Wright and Miller* (1996). Positive variations through time represent increased mantle plume activity under Iceland. (b) Rate of lava accumulation for several of the thick sections of radiometrically dated lava sequences on Iceland (*Saemundsson et al.*, 1980; *MacDougall et al.*, 1984; *Saemundsson*, 1986). The data are summarized in *Saemundsson* (1986). (c) Ages and thicknesses of ash layers found at ODP Site 907 which lies to the north of Iceland (*Mehyre et al.*, 1995). (d) Age of intervals with volcanic components at DSDP Site 407 (diagonal pattern) and 408 (gray shading) (*Luyendyk et al.*, 1979). (e) History of Northern Component water inferred from carbon isotope records (after, *Wright and Miller*, 1996).

waters. Therefore, deepwater masses proximal to source regions have high DIC $\delta^{13}C$ values and low nutrients, while more distal water masses have low DIC $\delta^{13}C$ values and high nutrients. Benthic foraminiferal $\delta^{13}C$ records can be used to reconstruct these patterns because certain benthic foraminifera accurately record $\delta^{13}C$ variations in the DIC reservoir (Belanger et al., 1981; Graham et al., 1981). By comparing benthic foraminiferal $\delta^{13}C$ values at various points in the deep ocean, one can determine deepwater patterns.

The late middle Miocene to Recent phase of NCW production is established by several lines of independent evidence. Interbasinal comparisons of benthic foraminiferal $\delta^{13}C$ values show that the Atlantic recorded higher values than those in the Pacific since ~12 Ma, indicating that the North Atlantic was proximal to a deepwater source (Fig. 9.4) (Miller and Fairbanks, 1985; Woodruff and Savin, 1989; Wright et al., 1991, 1992; Wright and Miller, 1996). The beginning of this large interbasinal $\delta^{13}C$ difference was associated with the development of seismic Reflector Merlin throughout the western North Atlantic region (Mountain and Tucholke, 1985). Similarly, Shor and Poore (1979) noted a prominent hiatus between 13 and 10 Ma at DSDP sites drilled to the south of Iceland and on the Rockall Plateau (Legs 48 and 49) (Fig. 9.4). Sedimentation on the Hatton and Snorri drifts increased between 13 and 12 Ma, in response to increased deepwater circulation (Miller and Tucholke, 1983; Wold, 1994). Northern Component Water fluxes have varied over the past 12 m.y. Brief interruptions during the late Miocene occurred around 9 and 7 Ma (Wright et al., 1991; Wright and Miller, 1996) and an unusually high NCW production existed during the Pliocene prior to the development of glacial-interglacial cycles (Fig. 9.4) (Shor and Poore, 1979; Raymo et al., 1992; Wright and Miller, 1996).

The controversy over the early to early middle Miocene NCW history (24–15 Ma) may be related more to the region of emphasis in each study. Woodruff and Savin (1989) concentrated their efforts on reconstructing the Pacific and Indian Ocean circulation patterns, while Wright et al. (1991, 1992) focused much of their attention in the Atlantic basins. Accordingly, Woodruff and Savin (1989) demonstrated the existence of an intermediate to upper deepwater mass that appears to have originated in the northern Indian Ocean, but found little evidence for NCW production prior to 12 Ma. Those authors postulated that the Indian Ocean water mass was warm and very saline, transporting heat to the high southern latitudes during the early and middle Miocene. Conversely, Wright et al. (1991, 1992) focused on deepwater changes in the North Atlantic during the Neogene. Except for a brief interval of NCW production during the earliest Oligocene (Miller, 1992), the first major phase of NCW production began in the early Miocene around 20 Ma (Wright et al., 1992). This interval lasted for ~4 m.y., reaching peak production around 17 Ma (Fig. 9.4). Seismic Reflector R2 has been traced to the Greenland-Scotland Ridge (Miller and Tucholke, 1983) and was attributed to this phase of NCW (Miller and Fairbanks, 1985). Age estimates for Reflector R2 vary, but fall in the interval between 20 and 16 Ma (Miller and Tucholke, 1983; Mountain and Tucholke, 1985; Bauldauf, 1987). Sites 406 and 407 also recorded a hiatus between 18 and 16 Ma that corresponds to this interval of NCW production (Fig. 9.4) (Shor and Poore, 1979). An important phase of drift accumulation in the North Atlantic began at this time (Jones et al., 1970; Ruddiman, 1972; Wold, 1994). Vogt (1972) cited this sedimentary evidence as support for his hypothesis that a critical depth along the Greenland-Scotland Ridge was reached during the early Miocene.

The phase of long-term NCW production that began during the late middle Miocene is consistent with both the simple thermal subsidence and dynamic mantle plume models (e.g., Schnitker, 1980; Wright and Miller, 1996). Both models predict that the Greenland-Scotland Ridge would subside to a critical depth to allow NCW to flow into the northern North Atlantic during the late middle Miocene. In contrast, the early to early middle Miocene phase of NCW production requires that the "critical" depths along the sill were reached several million years before the timing predicted by simple thermal subsidence models or that sill depths along the Greenland-Scotland Ridge have been more variable.

Wright and Miller (1996) argued that the correlation of inferred variations on the Greenland-Scotland Ridge with NCW production during the Neogene implied that sill depths on the ridge are an important control for deepwater circulation patterns. However, sediments recovered from the

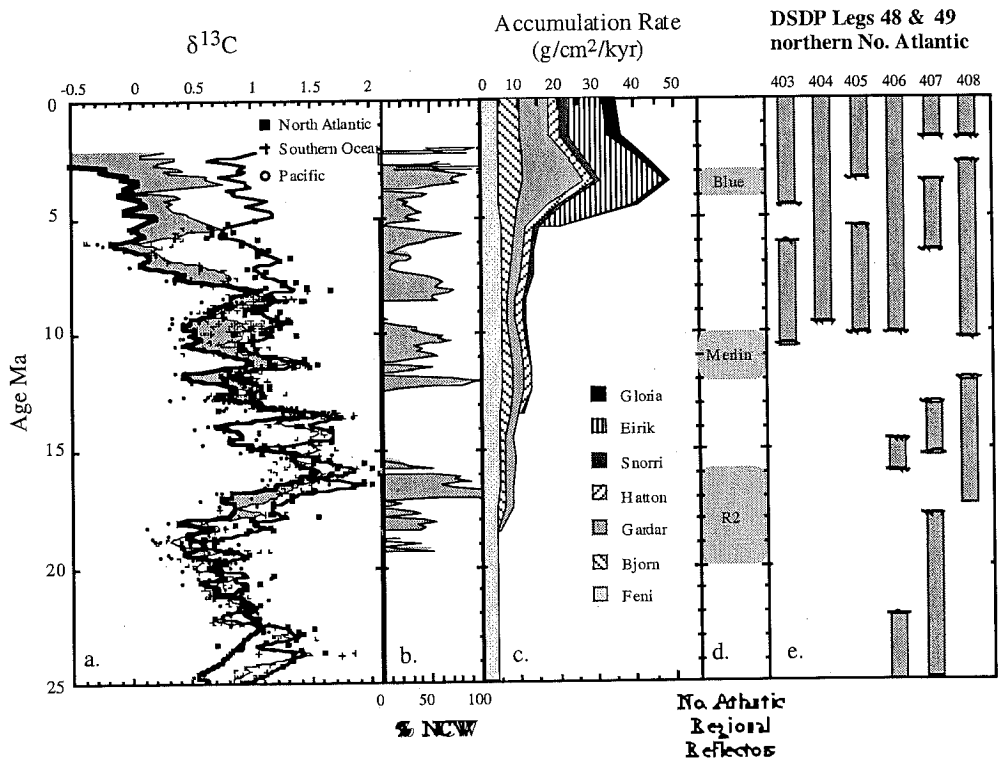

Fig. 9.4. (a) Composite $\delta^{13}C$ curves of the North Atlantic, Southern, and Pacific Oceans for the Neogene (after *Wright and Miller*, 1996). The shaded area represents times when the Southern Ocean $\delta^{13}C$ value was higher relative to the Pacific $\delta^{13}C$ value, indicating NCW production. (b) The record of Northern Component Water flux over the past 25 Ma estimated by recording the benthic foraminiferal $\delta^{13}C$ changes in the Southern Ocean relative to change in the North Atlantic and Pacific records. (c) Summary of the accumulation of drift sediments in the North Atlantic taken from *Wold* (1994). (d) Reflectors R2, Merlin, and Blue are three major seismic reflectors in the North Atlantic and their age ranges are shown on the side of the graph (*Mountain and Tucholke*, 1985). (e) Summary of sedimentation at sites drilled on DSDP Legs 47 and 48 (*Shor and Poore*, 1979). Note the major hiatuses in the early an middle Miocene which correspond to the major phases of NCW production.

Norwegian-Greenland Seas on DSDP Leg 38 and ODP Legs 151 and 152 are equivocal about deep ventilation in this region prior to 10 Ma (Talwani et al., 1976; Larsen et al., 1994; Thiede and Myhre, 1996). Another consideration is that Labrador Sea Water is an important component in modern NADW that forms south of the ridge; thus the formation of Labrador Sea Water may be invoked to explain this discrepancy. However, the distribution of sediment drifts and seismic disconformities implicates the Norwegian and Greenland Seas as a source of NCW during the Miocene (Ruddiman, 1972; Roberts, 1975; Shor and Poore, 1979; Miller and Tucholke, 1983; Vogt and Tucholke, 1989).

Another potential control on the Greenland-Scotland Ridge overflow is glacio-eustatic sea level changes which would effectively raise or lower sill depths along the ridge relative to sea level. Thiede and Eldholm (1983) noted that sea level changes could influence the exchange of water across the ridge particularly when sill depths along the ridge were not as deep. Haq et al. (1987) estimated that Miocene sea level events ranged between 50 and 150 m. More recent estimates suggest that the maximum sea level lowerings were no larger than 100 m with most Neogene sea level events ranging between 30 and 80 m below the present level (Greenlee and Moore, 1988; Miller et al., 1996). Wright et al. (1992) and Wright and Miller (1996) noted that NCW production during the early and middle Miocene was not constant and that flux changes could be related to sea level changes affecting the

overflow across the Greenland-Scotland Ridge.

Tectonic uplift/subsidence along the Greenland-Scotland Ridge and glacio-eustatic sea level changes focus on changes at the gateway that may isolate the probable source region for NCW (Greenland-Norwegian Seas) from the open North Atlantic. However, another potential influence on NCW production relates to the pre-conditioning of surface waters that sink to form NCW. High salinity is necessary for the formation of NCW (Reid, 1979). The surface and thermocline waters that flow into the Nordic Seas acquire high salinities as they flow through tropical and subtropical Indian and Atlantic Oceans. This inter-ocean exchange of surface and thermocline waters is part of a global system that circulates surface and deep water among all of the ocean basins (e.g., Gordon, 1986; Broecker and Denton, 1990). A critical gateway in this circulation system may be the Central American Isthmus. Results from ocean modeling experiments indicate that with an open isthmus, low salinity water from the Pacific enters the North Atlantic, making it difficult for NCW to form (Maier-Reimer et al., 1990; Mikolajewicz et al., 1993). This author recognizes the importance of this aspect, but assumes for this discussion that the surface waters that flowed into the Greenland-Norwegian Seas were sufficiently pre-conditioned to sink with heat loss to the atmosphere and form a deepwater mass.

DeepWater and Climate Change

The most recent glacial to interglacial transition provides the best illustration for how changes in deepwater circulation patterns in the North Atlantic may have affected climate. At present, the NADW production is high and temperatures in the circum-North Atlantic (both marine and terrestrial) are relatively warm. In contrast, NCW production was much lower during the most recent glacial maximum at ~20 to 18 ka (e.g., Oppo and Fairbanks, 1987; among many) and sea surface temperature (SST) estimates indicate 6 to 10°C cooler waters accompanied by large ice sheets on the adjacent continents (CLIMAP, 1981). The relationship of high NCW during interglacials and low NCW during glacials has been extended into the Pliocene (Oppo et al., 1990; Raymo et al., 1990, 1992). The argument that climate responds to deepwater circulation changes is compelling; however, whether NCW is a primary cause for climate change or just a consequence of climate change is still in doubt. For example, Broecker and Denton (1990) argue that the late Pleistocene climate cycles are a result of thermohaline reorganizations. In contrast, Raymo et al. (1992) attribute a decrease in NCW production during the late Pliocene to the increase in Northern Hemisphere glaciation.

Neogene Climates

Neogene climates are most often and best characterized by benthic foraminiferal $\delta^{18}O$ records (e.g., Savin et al., 1975; Shackleton and Kennett, 1975; Miller et al., 1987). The most prominent feature is the middle Miocene $\delta^{18}O$ increase of > 1 ‰ that is recorded throughout the intermediate and deep oceans between 15 and 12.8 Ma (Fig. 9.5). This increase has been attributed to the development of a permanent ice sheet on Antarctica (Shackleton and Kennett, 1975) with accompanying deepwater cooling (Savin et al., 1975; Shackleton and Kennett, 1975; Miller et al., 1987; Wright et al., 1992). The timing of the permanent ice cap on Antarctica is in question as there is extensive evidence for Antarctic glaciation during the late Eocene and Oligocene (Barron et al., 1991; Miller et al., 1991; Schlich et al., 1992; Zachos et al., 1993). However, it remains unclear whether these Paleogene ice sheets were permanent or intermittent.

Northern Component Water has been implicated as a possible cause for the middle Miocene $\delta^{18}O$ increase. Schnitker (1980) related the middle Miocene $\delta^{18}O$ increase to the initiation of NCW formation during the middle Miocene. He proposed that the upwelling of warm NCW around Antarctica increased the moisture flux to Antarctica, causing large ice sheets to grow. Wright and Miller (1996) noted the coincidence in timing of the NCW shutdown between 16 and 15 Ma and the beginning of the middle Miocene $\delta^{18}O$ increase at 15 Ma. The timing of these deepwater and climate changes are well-constrained with paleomagnetic data (Wright et al., 1992). However, they concluded that the delay between NCW shutdown (16 to 15 Ma) and culmination of the climate change (12.8 Ma) was too long for the reduction in NCW to have been the primary cause. Wright and Miller (1996) suggested that the NCW production warmed the high-latitude climates,

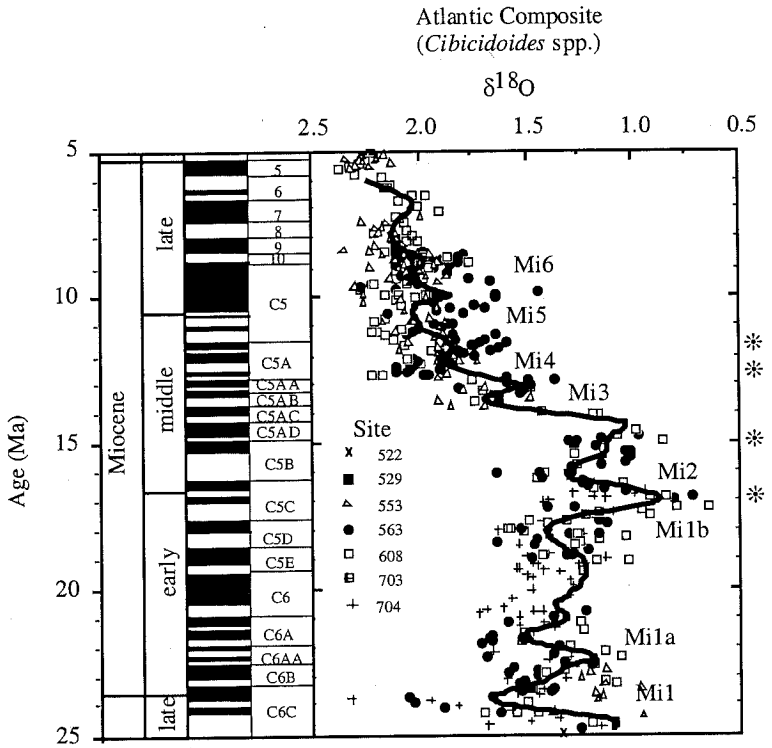

Fig. 9.5. Benthic foraminiferal $\delta^{18}O$ curve for the Neogene modified from *Wright and Miller* (1993). The solid line was generated by interpolating the data to constant intervals of 0.5 million years and smoothing with an 11 point gaussian filter. The "Mi" glacial events identified by *Miller et al.* (1991) are shown. The middle Miocene $\delta^{18}O$ increase began around 15.0 Ma and culminated with a $\delta^{18}O$ maximum at 12.8 Ma. The *Berggren et al.* (1995) time-scale was used. Asterisks denote times used for equator to pole reconstructions.

but its shutdown was not primarily responsible for the long-term climate changes. Other hypotheses to explain the middle Miocene $\delta^{18}O$ increase include: the Monterey hypothesis of carbon sequestering in isolated basins removing CO_2 from the atmosphere (Vincent et al., 1985); and continent–continent collisions and arc-continent collisions disrupting the carbon cycle which also led to the removal of CO_2 from the atmosphere [e.g., Himalayas (Raymo and Ruddiman, 1992; Raymo, 1994), Indonesia-New Guinea (Reusch and Maasch, this volume, Chapter 13)]. One problem with these carbon cycle models may be the delay in the removal of carbon as indicated by the increase oceanic $\delta^{13}C$ values from 20 to 16 Ma and the beginning of the middle Miocene $\delta^{18}O$ increase around 15 Ma (Hodell and Woodruff, 1994).

Surface Water Reconstructions

One potential measure of the effects of deepwater circulation change on climate during the Neogene may lie in the SST gradients measured at times of contrasting deepwater circulation patterns. Gradients based on planktonic foraminiferal $\delta^{18}O$ values provide the best information regarding paleo-SST gradients (Shackleton and Boersma, 1981; Keller, 1985; Savin et al., 1985; Zachos et al., 1994; among others). However, temperature is not the sole influence on the modern $\delta^{18}O_{calcite}$ gradient. All paleotemperature equations include the $\delta^{18}O_{water}$ term (e.g., Epstein et al., 1953).

$$T = 16.5 - 4.3\,(\delta^{18}O_{calcite} - \delta^{18}O_{water}) + 0.14\,(\delta^{18}O_{calcite} - \delta^{18}O_{water})^2 \qquad (9.2)$$

where T and $\delta^{18}O_{water}$ are the temperature (°C) and oxygen isotope value of the water in which the organism lived, and $\delta^{18}O_{calcite}$ is the oxygen isotope value measured in the calcite. From this equation, there is a one-to-one relationship between changes in $\delta^{18}O_{calcite}$ and $\delta^{18}O_{water}$ values. In contrast, there is an inverse relationship between $\delta^{18}O_{calcite}$ and temperature such that for every 1°C temperature increase there is a 0.23‰ decrease in the measured $\delta^{18}O_{calcite}$ value.

The key to using planktonic foraminiferal $\delta^{18}O$ values as indicators of past climates is understanding the hydrographic parameters which produce the modern $\delta^{18}O_{calcite}$ gradient. In the modern ocean, the predicted meridional $\delta^{18}O_{calcite}$ gradient (equator to pole) is greater than 5.0 ‰ and is dominated by temperature changes (~28°C). Therefore, it is tempting to ascribe planktonic foraminiferal $\delta^{18}O$ gradients to temperature differences alone. The importance of the $\delta^{18}O_{water}$ term is highlighted when we consider that surface water $\delta^{18}O_{water}$ values vary by ~1.5 ‰ (equivalent to a 6–7°C temperature effect) with high values in the tropics and subtropics and the lowest values in the polar regions. This variation is due to the general transport of water vapor from low (evaporation) to high latitudes (precipitation). During this process, the $\delta^{18}O$ value of the water vapor decreases through a distillation process (Craig and Gordon, 1965). Hence, the precipitation in the polar/subpolar regions has lower $\delta^{18}O$ values than in the tropics/subtropics. These differences affect the oceanic environment because the $\delta^{18}O$ values at various points in the ocean represent mixing between the more saline, high $\delta^{18}O$ waters in the evaporative regions of the oceans (subtropics) and the fresh, low $\delta^{18}O$ riverine water (Craig and Gordon, 1965). As a result, planktonic foraminiferal $\delta^{18}O$ gradients must be evaluated as a gradient which incorporates both temperature and $\delta^{18}O_{water}$ values (e.g., Savin et al., 1985) .

Zachos et al. (1994) minimized the errors associated with not knowing the $\delta^{18}O_{water}$ term for the early Cenozoic oceans by using the modern $\delta^{18}O_{water}$ gradient. However, the $\delta^{18}O_{water}$ variations in the ocean are linked to climate and certainly differed in the past. First-order comparisons must be made based on $\delta^{18}O$ values alone. Any subsequent interpretation requires a firm knowledge of either the temperature or $\delta^{18}O_{water}$ term. In this chapter, $\delta^{18}O$ measurements of coretop planktonic foraminifera, sampled along a meridional transect in the North Atlantic, are compared with similar transects representing four Miocene time slices. This method is similar to that of Savin et al. (1985) and provides first-order approximation for surface hydrographic changes.

Planktonic Foraminiferal Equator to Pole Transects in the North Atlantic

Stable isotopic values were determined for the most abundant planktonic foraminiferal taxa at four stratigraphic levels in seven DSDP sites. These sites formed a south to north transect near the Mid-Atlantic Ridge that spans 5–63°N in latitude (Table 9.1). These equator-to-pole transects in the North Atlantic were selected to characterize the surface water hydrographic changes that may have resulted from changes in NCW production. To ensure time equivalence, each transect selected was associated with a distinct benthic foraminiferal $\delta^{18}O$ event, which are assumed to be synchronous (Miller et al., 1991). The Berggren et al. (1995) time-scale is used to determine the age of the surface water $\delta^{18}O$ transects. All analyses for the Miocene transects were run in the Stable Isotope Laboratory at the University of Maine. Precision on the NBS-20 standards during the analyses was 0.06 and 0.05‰ for $\delta^{18}O$ and $\delta^{13}C$, respectively.

The presence of high-frequency climate cycles (40 kyr) during the middle Miocene (Pisias et al., 1985; Flower and Kennett, 1995) can potentially introduce error into the comparisons used in this study because the downcore records, from which the time slices were chosen, were under-sampled. The sample resolution used in this study varies between 20 and 50 kyrs depending on the site. Unlike the late Pleistocene when glacial/interglacial cycles record an amplitude of ~2.0 ‰, the middle Miocene cycles are approximately one third to one-quarter of this amplitude (0.5–0.6‰), minimizing the magnitude of potential errors associated with low sample resolution.

Middle Miocene $\delta^{18}O$ *Transects*. The potential for NCW to influence middle Miocene climates is evaluated by comparing the meridional $\delta^{18}O$ gradients reconstructed from planktonic foraminifera for time intervals slices which represent times when NCW

Table 9.1. Oxygen Isotope Values Used in the Composite $\delta^{18}O$. Transects Shown in Fig. 9.6

Site	Latitude (°N)	Species	Core	Section	Interval	$\delta^{18}O$
			17 Ma Time Slice			
667A	5	*D. altispira*	21	4	40	-1.14
667A	5	*G. ruber*	21	4	40	-1.51
667A	5	*G. sacculifer*	21	4	40	-1.34
366	6	*D. altispira*	20	2	130	-1.38
563	34	*D. altispira*	11	3	19	-0.75
408	63	*G. praebulloides*	34	6	75	0.52
			15 Ma Time Slice			
667A	5	*D. altispira*	19	5	36	-1.33
667A	5	*G. sacculifer*	19	5	36	-1.23
667A	5	*G. sacculifer*	19	5	36	-1.44
563	5	*D. altispira*	9	4	25	-0.88
563	5	*D. altispira*	9	4	25	-0.52
608	43	*G. mayeri*	34	4	105	-0.49
608	43	*D. altispira*	34	4	105	-0.01
408	63	*G. praebulloides*	32	2	142	0.57
			12.8 Ma Time Slice			
667A	5	*D. altispira*	18	2	36	-0.61
667A	5	*G. mayeri*	18	2	36	-0.54
667A	5	*G. ruber*	18	2	36	-0.67
667A	5	*G. sacculifer*	18	2	36	-0.68
366A	6	*D. altispira*	15	6	116	-0.58
563	34	*D. altispira*	8	1	34	0.68
608	43	*G. bulloides*	31	1	85	1.03
608	43	*D. altispira*	31	1	85	0.67
553	56	*G. bulloides*	7	6	80	0.98
553A	56	*G. bulloides*	7	6	80	0.69
553A	56	*G. mayeri*	7	6	80	0.99
553A	56	*G. mayeri*	7	6	80	0.69
553A	56	*G. peripheroronda*	7	6	80	0.21
408	63	*G. bulloides*	27	5	86	1.89
			11.8 Ma Time Slice			
366A	6	*D. altispira*	15	3	122	-0.39
563	34	*D. altispira*	5	4	110	0.26
563	34	*G. nepenthes*	5	4	110	0.55
563	34	*G. nepenthes*	5	4	110	0.60
608	43	*D. altispira*	27	7	11	1.04
608	43	*D. altispira*	27	7	11	1.10
608	43	*G. bulloides*	27	7	11	0.96
608	43	*G. bulloides*	27	7	11	1.06
608	43	*G. mayeri*	27	7	11	0.26
608	43	*G. mayeri*	27	7	11	0.12
407	63	*G. bulloides*	17	3	84	1.23
408	63	*G. bulloides*	24	6	0	1.55

was "on" and "off." Two comparisons were made, representing of NCW change before and after the middle Miocene $\delta^{18}O$ increase. Time slices for both comparisons were selected based on the similarity of benthic foraminiferal $\delta^{18}O$ values. This criterion minimizes the possibility that other factors may overprint the effects of NCW changes.

Transects for time slices at 17 Ma and 15 Ma were constructed to represent surface conditions prior to the middle Miocene $\delta^{18}O$ increase and were chosen as follows: the $\delta^{18}O$ minima before and after the Mi2 event, respectively (Miller et al., 1991). The absolute values for the 17 Ma and 15 Ma time slices are similar and are interpreted to reflect otherwise similar climatic conditions (Fig. 9.5) (Wright et al., 1992). The key difference between the two time slices is that NCW production decreased from peak production at ~17 Ma to undetectable levels by 15 Ma (Wright et al., 1992). Although based on only a few points, the $\delta^{18}O$ transects for the 17 Ma and 15 Ma time slices are similar. This indicates that changes in the flux of NCW had little effect on the $\delta^{18}O$ transect during the early middle Miocene, and hence, North Atlantic surface water hydrography (Fig. 9.6). If SST changes did occur, they would have been offset exactly by changes in $\delta^{18}O_{water}$ values, a less plausible scenario.

A similar comparison using the 12.8 Ma and 11.8 Ma transects is made to examine surface water changes associated with the re-initiation of NCW production during the late middle Miocene. Transects for 12.8 Ma and 11.8 Ma time slices postdate the middle Miocene $\delta^{18}O$ increase and represent times when NCW was beginning to re-establish (12.8 Ma) and when there was a significant flux (11.8 Ma) (Woodruff and Savin, 1989; Wright et al., 1992). These two time slices correspond to the Mi4 and Mi5 events of Miller et al. (1991). Benthic foraminiferal $\delta^{18}O$ values at 12.8 and 11.8 Ma were similar to the modern value indicating that deepwater temperatures were close to modern values during the late middle Miocene (Savin et al., 1975; Shackleton and Kennett, 1975; Miller et al., 1987). As in the case before the middle Miocene $\delta^{18}O$ increase, there is little difference between the 12.8 Ma and 11.8 Ma profiles, indicating no substantial change in surface water conditions associated with the initiation of and increase in NCW production during the late middle Miocene (Fig. 9.6).

Discussion

The two most prominent climate changes during the Neogene are the middle Miocene $\delta^{18}O$ increase and the development of large-scale North Hemisphere glaciation during the late Pliocene. Each climate event corresponded to a large-scale change in NCW production (Wright et al., 1992; Wright and Miller, 1996). Sediments from ODP Leg 151 show evidence for small-scale Northern Hemisphere glaciation at 14 and 13 Ma (Wolf-Welling et al., 1996), which corresponds to the Mi3 and Mi4 events recorded in the $\delta^{18}O$ record (Miller et al., 1991; Wright et al., 1992). It remains to be shown whether the initiation of the middle Miocene $\delta^{18}O$ increase at 15 Ma corresponded to a phase of Northern Hemisphere glaciation. If so, then a direct cause and effect can be made between the NCW decreases and the development of Northern Hemisphere ice sheets. A similar climate–deepwater relationship is observed for the Pliocene. Warm climates occurred when NCW fluxes were high during the early Pliocene (Raymo et al., 1992; Wright and Miller, 1996). By the late Pliocene (3.2 Ma), NCW production decreased and large-scale Northern Hemisphere glaciation commenced. In each case, it may be argued that reduced delivery of heat to the high northern latitudes precipitated the development of Northern Hemisphere ice sheets.

The coincidence between Northern Hemisphere glaciation and NCW decreases is intriguing; however, the timing and magnitude of change in this interval indicates that other changes in the ocean–atmosphere system must have accompanied the NCW changes to account for the long-term climate coolings. For example, the decrease in NCW flux occurred between 16 and 15 Ma and yet the $\delta^{18}O$ increase ended at 12.8 Ma, requiring too long a delay to account for the climate change (Wright and Miller, 1996). This conclusion is further supported by the similarity of the $\delta^{18}O$ transects at 17 Ma and 15 Ma and those at 12.8 Ma and 11.8 Ma; both compare surface water conditions at times of contrasting fluxes of NCW (Fig. 9.6). Despite large-scale deepwater changes, the surface waters recorded